

RC 19348 (84143) 1/10/94
Chemistry 28 pages

Research Report

Modeling and Response Surfaces for Electroless Co Deposition Process

Milan Paunovic

IBM Research Division
T. J. Watson Research Center
Yorktown Heights, NY 10598

Trang Nguyen

IBM Storage Systems Division
San Jose, CA 95120

Ruby Mukherjee, Carlos Sambucetti and Lubomyr T. Romankiw

IBM Research Division
T. J. Watson Research Center
Yorktown Heights, NY 10598

LIMITED DISTRIBUTION NOTICE

This report has been submitted for publication outside of IBM and will probably be copyrighted if accepted for publication. It has been issued as a Research Report for early dissemination of its contents and will be distributed outside of IBM up to one year after the date indicated at the top of this page. In view of the transfer of copyright to the outside publisher, its distribution outside of IBM prior to publication should be limited to peer communications and specific requests. After outside publication, requests should be filled only by reprints or legally obtained copies of the article (e.g., payment of royalties).

MODELING AND RESPONSE SURFACES
FOR ELECTROLESS Co DEPOSITION PROCESS

Milan Paunovic, Trang Nguyen*, Ruby Mukherjee, Carlos Sambucetti,
and Lubomyr T.Romankiw

IBM T.J.Watson Research Center
Yorktown Heights, New York

*IBM Storage Systems Division, San Jose, California

ABSTRACT

The electroless deposition process was studied by statistical techniques using IBM Storage Systems Division statistical computer program ADOE (Automatic Design Of Experiments). Three types of experiments were designed: the two-factor two-level factorial, the two-factor three-level factorial, and the central composite rotatable five-factor five-level experiments. The two-factor factorial experiments were used to determine the effect of each individual variable (factor) and interactions between variables. It was concluded from the analysis of data that (i) the most significant factors are citrate, the Co^{2+} complexing agent, pH, and temperature, and (ii) the most significant interactions are pH-citrate, pH-hypophosphite, and citrate-boric acid interactions. The central composite rotatable experiments were used to construct the second-order empirical model for the relationship between the Co deposition rate and five independent variables. The interpolation polynomial had 21 coefficients. The interpolation function was used to construct the 3-D response surfaces and 2-D response contours. Two types of response surfaces were found: simple maximum and rising ridge. The interpolation polynomial was used also to optimize the Co deposition process with respect to the minimized variability.

INTRODUCTION

The effect of process variables on the rate of deposition and properties of electrolessly deposited metals is usually studied by one-factor-at-a-time experiments (one-factor experiments in the further text). In these experiments the effect of a single variable (factor), e.g. x_1 , in the multivariable process with the response y , $y = f(x_1, x_2, x_3, \dots, x_n)$, is studied by varying the value (level) of this variable while holding the values of the other independent variables fixed, $y = f(x_1)_{x_2, x_3, \dots, x_n}$. This process is repeated with other variables until the effect of each variable on the response y (e.g. $y =$ rate of deposition, or $y =$ a property of the deposit) has been examined. Thus, in these experiments the effect of one variable on the response y is determined at only one level of other variables. Any prediction (extrapolation) of the effect of a single variable on the response y at the different level of other variables, made on the basis of these one-factor experiments, implies the assumption that the effect of one variable is independent of levels of the other variables. However, in many cases the effect of one variable depends on the level of other variables. This dependence is due to the interaction between variables which is frequent in chemical and electrochemical processes.

Interactions between variables can be easily detected by use of the factorial design of experiments. In a full factorial design a fixed number of levels for each variable is selected and then experiments are run with all possible combinations of variables and levels. Thus, in the factorial experiments the effect of a factor is estimated at several levels of the other factors and the results are valid over a range of experimental conditions (1). Factorial designs at two levels are used in preliminary experimental work. Designs of the higher degree of complexity are used for study of functional relationships between response and independent variables, modeling, and process optimization.

Our objective in this work is to apply the above statistical techniques to electroless deposition of cobalt in order to detect interactions between variables, build a model of the process, construct response surfaces and response contours, and optimize the electroless deposition process. The rate of electroless cobalt deposition is a function of at least ten variables. The application of the multifactor experimental design to this process results in very useful information for the process, process control, and process optimization. We present results

in four sections: two-factor two-level model, two-factor three-level model, one-factor experiments, and five-factor five-level model.

EXPERIMENTAL

Electroless solutions were prepared with analytical grade reagents and distilled water. The complexing agent for Co^{2+} ions in the electroless deposition solution was citrate ion ($\text{C}_6\text{H}_5\text{O}_3^-$), the buffer was boric acid (H_3BO_3), NaOH to pH 8.00, the reducing agent was sodium hypophosphite ($\text{NaH}_2\text{PO}_2 \cdot \text{H}_2\text{O}$) and the source of Co^{2+} ions was $\text{CoSO}_4 \cdot 7\text{H}_2\text{O}$. Deposition was carried out for 30 minutes. The rate was determined by the weight gain method. The substrate was evaporated or sputtered Cu (5000 Å) on a silicon wafer (3.2 cm diameter) covered with Cr (400 Å) adhesion layer. Prior to electroless deposition the Cu surface was cleaned in 20% H_2SO_4 and H_2O and activated with PdCl_2 solution. No agitation was used during the electroless Co deposition.

The design matrix for the two-factor two-level (2^2) experiments is shown in Table I. This matrix was chosen in order to determine interactions between factors and select factors for further designs of the higher degree of complexity. Table II shows the design matrix for the two-factor three-level (3^2) experiments. These three-level experiments can detect a curvature in the functional relationship between the response and independent variable. The design matrix for the five-factor five-level model is shown in Table III. This multilevel design is the central composite rotatable design that consists of three parts. The first part is the five-factor two-level 16-trial fractional factorial, 2^{5-1} , Fisher matrix. This matrix can estimate all main effects and all two-factor interactions. It is assumed that the higher interactions are negligible. A complete replicate of the 2^5 factorial design requires 32 experiments. By assuming that the three-factor interactions and higher are negligible considerable saving in experimentation is achieved. The second part consists of 10 star points 3-level experiments. The third part consists of 6 center points where variables have the center value of the variable range. The complete central composite design can determine curvature to all variables and thus was used for model building and construction of response surfaces.

The analysis of experiments was done by IBM Storage Systems Division statistical computer program ADOE (Automatic Design Of Experiments).

RESULTS

Two-Factor Two-Level Factorial Design (2²)

Fig.1 shows the interaction graph for citrate and pH. The intersecting lines indicate strong interaction between these variables. According to Fig.1a the pH has a significant effect on the rate of deposition, but it depends on the level of citrate concentration. At the low concentration of citrate (30 g/L) the effect of pH is negative, i.e. the rate of deposition decreases with the increase in pH. At the high concentration of citrate (100 g/L) the effect of pH is positive, i.e. the rate of deposition increases with the increase in pH. This is opposite to the pH effect at the low concentration of citrate. Thus, the sign and the magnitude of the slope $\partial r/\partial \text{pH}$, where r is the rate of deposition, change with the concentration of citrate. Fig.1 (a and b) shows that the effect of citrate is negative at both pH values, pH 7.75 and 8.20; that is, the rate of deposition decreases with the increase of the citrate concentration. However, the magnitude of the slope of this change, $\partial r/\partial c$, is a function of pH and decreases as pH increases. Fig. 2 shows the analysis of means plot for the effects of factors and interaction for the same design. This graph shows that the strongest effects are the effect of citrate and the effect of the interaction between citrate and pH. Also, it shows that if the objective is the maximum rate one should select the low concentration of citrate (30 g/L) and the low pH (7.75) since this combination results in the highest rate.

The analysis of means plot was constructed using the linear statistical model with interaction between factors (1)

$$y_{ijk} = \mu + \tau_i + \beta_j + (\tau\beta)_{ij} + \varepsilon_{ijk}$$

where i (level of factor A) = 1,2; j (level of factor B) = 1,2; k (replicate number) = 1,2; μ -the overall mean (a common parameter, $\mu = \sum y_{ijk}/k$); τ_i -the effect of the i th level of the factor A; β_j -the effect of the j th level of the factor B; $(\tau\beta)_{ij}$ -the interaction between τ_i and β_j ; ε_{ijk} -a random error component. Decision lines (DL) were computed using equation

$$DL(Y) = \bar{y} \pm H_\alpha \frac{\hat{\sigma}_y}{\sqrt{n}}$$

where \bar{y} is the grand mean ($\bar{y} = \sum_{i=1}^k \bar{y}_i/k$; \bar{y}_i is the sample mean), H_a is Ott's factor for analysis of means, α is degree of risk, σ the standard deviation, and n the sample (subgroup) size (2).

Two-Factor Three-Level Factorial Design (3²)

The interaction between citrate and boric acid was tested by the two-factor three-level (3²) experiments. Fig.3 shows the interaction graph and Fig.4 shows effects of factors and interaction between factors. One can see from Figs.3 and 4 that there is a strong interaction between citrate and boric acid and that the effect of boric acid is a function of concentration of citrate (Fig.3). As in pH effect, at low concentration of citrate the rate decreases with the increase in the boric acid concentration, and at the high concentration of citrate the rate increases with the increase of concentration of boric acid. The analysis of variance on mean is given in Table IV. Table IV and Fig.4 show that the effect of citrate (A) and the effect of the AB² component of the citrate (A)-boric acid (B) interaction are the most important effects.

One-Factor Experiments

The rate of deposition as a function of pH and temperature was examined in one-factor experiments. Fig.5 shows that the pH effect depends on the concentration of citrate. The rate as a function of pH first increases, reaches a maximum, and then decreases with the increase in pH. Fig.6 shows that the rate as a function of temperature follows the Arrhenius behaviour.

Central Composite Rotatable Design

Three types of results were obtained using this design: (i) effects of main factors and two-factor interactions, (ii) the empirical second order model, and (iii) response surfaces (1).

Effects . Analysis of means plots and interaction graphs show that the most significant factors are citrate and temperature and the most significant interactions are pH-citrate and pH-hypophosphite interactions.

The empirical second order model. Results of the central composite rotatable design experiments and the regression analysis were used to determine the constant (β_0), the coefficients of linear terms (β_i), the coefficients of quadratic terms (β_{ii}), and the coefficients of the mixed terms (β_{ij}) in the second order polynomial (3-5).

The approximating polynomial (the least-square estimated value of y) \hat{y} for the functional relationship between the response y and k independent variables (coded) x_1, x_2, \dots, x_k is given by

$$\hat{y} = \hat{\beta}_0 + \sum_{i=1}^k \hat{\beta}_i x_i + \sum_{i=1}^k \hat{\beta}_{ii} x_i^2 + \sum_i \sum_{j \substack{< \\ i < j}} \hat{\beta}_{ij} x_i x_j$$

where $\hat{\beta}$ coefficients are the least-square estimated β coefficients. Estimated coefficients for the approximating polynomial are shown in Table V. The model was checked by evaluating residuals and the R^2 statistic (the coefficient of determination or regression coefficient)

$$R^2 = \frac{\sum (\hat{y}_i - \bar{y})^2}{\sum (y_i - \bar{y})^2}$$

$$R^2 = \frac{SS_{\text{Regression}}}{SS_{\text{Total}}}$$

where \bar{y} is the sample mean response, and SS the sum of squares (1,5). For the present polynomial $R^2 = 0.933$; $R^2 = 0$ means that the data are random noises and $R^2 = 1$ means that the data are exactly on the polynomial. Thus, $R^2 = 0.933$ means that 93.3 percent of variability in the data is accounted for the model.

Response surfaces and process optimization. The approximating polynomial obtained on the basis of the central composite design experiments and the regression analysis, as described above, was used to obtain response surfaces.¹¹ Two types of response surfaces (RS) were found: simple maximum and rising ridge. RS classified as simple maximum can be of two types: the maximum is in the experimental range and the maximum is outside of the experimental range. Two modes of RS presentation were used: (i) fixed variables (3 not plotted variables in this case) are at the center of the experimental region and (ii) fixed variables are at the point of the minimum variability.

A method of ridge analysis (1,3) is used to find the minimized variability points within the experimental region. Since the variability of the response is caused by the variability of the factors and the slope of the response surface the first order Taylor approximation is used to write the variance of the response (here the rate of deposition) as a function of slopes of the response surfaces and the variances of the factors (variables).

The experimental range, the center points, and the points of the minimum variability for variables are given in Table VI. Some response surfaces (RS) and contour plots in the first mode (the center of the experimental region) and the second mode (minimum variability) are shown in Figs. 7-9. A comparison of columns 3 and 4 in Table VI shows the recommended changes to be introduced in the values of process variables in order to minimize the variability in the rate of deposition. An analysis of response surfaces gives a graphical illustration of the range of the large variability and the range of the minimized variability. E.g., in the ridge type of RS the range of the minimum variability is the plateau on the top of the ridge and the range of the high variability is the sloping part of the RS.

DISCUSSION

Effect of pH as a function of citrate concentration. One of the most interesting and technologically most important findings in this work is the interaction between pH and citrate in the electroless Co deposition process. This interaction was easily discovered by the factorial design of experiments. Fig.1a shows that there are two types of pH effects in the examined pH range (pH 7.75-8.20). First, the effect of pH is positive at high concentration of citrate (100 g/L) and second, it is negative at the low concentration of citrate (30 g/L).

The first topic for discussion is the dependence of the sign of the pH effect on the concentration of citrate. Two basic explanations are possible. First, the sign is specific for a given range of citrate concentration. Second, the sign is not specific, and in general, both signs, positive and negative can be observed at any concentration of citrate. On the basis of known publications on the pH effect in electroless deposition (6-8) we can predict that the second case is the valid interpretation. To verify this hypothesis we have performed series of one-factor experiments and the results are shown in Fig.5. Fig 5 shows that the rate of deposition at first increases, reaches a maximum, and then decrease with the increase in pH. The location of the maximum depends on the concentration of citrate. Thus, in general, the positive and the negative sign of $\partial r/\partial \text{pH}$ can exist at any concentration of citrate. The position of the maximum is a function of pH and the concentration of citrate. Fig.5 also interprets results shown in Fig. 1a. The pH range tested in Fig. 1a is shown between dashed vertical lines in Fig.5. Thus, 2^2 factorial experiments see only one segment of the real rate = f(pH) function and according to this segment appears that the pH effect at 30 g/L of citrate is fundamentally different than that at 100 g/L citrate. One-factor experiments show that this difference is not fundamental but that 2^2 experiments look at two different sections of the same functional behaviour. This discussion illustrates importance of factorial experiments and one-at-a-time (one-factor) experiments.

The next discussion is on the elucidation of the negative and the positive segments of the rate = f(pH) curve. Since OH^- ions are reactants in the charge transfer step of the anodic partial reaction



one can consider that the positive pH effect is due to the anodic partial reaction. OH^- ions do not take part directly in the cathodic partial reaction; they can influence the cathodic partial reaction indirectly by entering the Co^{2+} coordination sphere and by double layer effects. Thus, it can be concluded that the positive pH effect is mostly a result of the increase in the concentration of the reactant OH^- in the partial anodic reaction. The negative pH effect could be explained on the basis of the pH effect on the (i) the structure of the coordination sphere of Co^{2+} ions and the structure of the double layer and (ii) the

electrochemical kinetic parameters (potential and the charge transfer coefficients α) of the anodic and the cathodic partial reactions. It was shown in the case of the electroless Cu deposition that the negative and the positive pH effects can be explained on the basis of the pH dependence of the charge transfer coefficients (8). Further discussion on this topic is out of scope of this paper.

Effect of boric acid as a function of citrate concentration. Results shown in Fig.3 and 4 are of technological importance since they show that the dependence of the rate of deposition on concentration of citrate can be minimized if a higher concentration of boric acid is used. At 20 g/L boric acid the rate of deposition significantly depends on concentration of citrate while at 35-50 g/L boric acid this dependence is much smaller. The interaction between boric acid and citrate is related to their complexing properties for Co^{2+} ions.

Empirical modeling and response surfaces. The empirical second order model and response surfaces are used to analyze the effect of set of independent variables x on the response y in the experimental region, to predict the response of the system to the variation in experimental conditions, and to optimize the process. In the electroless deposition process optimization can be with respect to the maximum response (y = rate of deposition) or with respect to the minimized variation in response due to variation in experimental conditions. One important example is variation in the rate of deposition with pH. Figs.1(a) and 5 show that there is a steep variation in rate with pH at the 30 g/L of citrate. It can be seen from the interaction graph, Fig.1(a), that this steep variation can be minimized by increasing concentration of citrate. A new set of 2^2 factorial experiments were performed in order to clarify this point and results are shown in Fig.10. These results clearly show the change of the slope $\frac{\partial r}{\partial \text{pH}}$ with the change in concentration of citrate. The same conclusions can be reached from the analysis of the response surfaces shown in Fig.9. Fig.11 shows the rate of deposition as a function of pH at various concentrations of citrate obtained from the second order polynomial (Table V). This polynomial is valid for the experimental range as given in Table VI, pH 7.75-8.25, and in Fig. 20 it is extended to the range 7.25-8.75 in order to illustrate this important dependence of the slope on the concentration of citrate. Since the range is extended the values of the rate of deposition do not correspond well to the experimental values. Thus, the polynomial curves (Fig.11) as well as the experimental

curves (Fig.5,9,10), show that the magnitude and the sign of the slope of $r = f(\text{pH})$ is a function of the concentration of citrate.

CONCLUSIONS

The major conclusions from this work are: (i) the use of statistical techniques to the study of the electroless Co deposition process resulted in the discovery of the interactions between different variables in the process and the discovery of new, so far unknown, characteristics of the pH effect in this process, (iii) the empirical second order model can be used for graphical analysis of the process by constructing response surfaces, for optimization of the process, and for predictions of the response (e.g. the rate of deposition) to the variation of process variables, and (iv) one-factor experiments (one variable-at-a-time) are usefull and necessary compliment to factorial design experiments as was demonstrated in the interpretation of the pH effect.

Acknowledgements

The authors gratefully thank to Michelle Cook and Sol Krongelb for the preparation of Cu/Cr seed layer.

This was Paper 546 presented at the New Orleans, Louisiana, Meeting of the Society, Oct. 10-15, 1993.

References

1. D.C.Montgomery, *Design and Analysis of Experiments* , John Wiley & Son, New York, 1984.
2. E.R.Ott and E.G.Schilling, *Process Quality Control* ,Mc.Graww-Hill Publishing Company, New York,1990.
3. G.E.P.Box and N.R.Draper, *Empirical Model-Building and Response Surfaces* ,J.Wiley & Sons, New York, 1987.
4. G.E.P.Box, W.G.Hunter, and J.S.Hunter, *Statistics for Experimenters* ,J.Wiley & Sons, New York, 1978.
5. D.C.Montgomery and E.A.Peck, *Introduction to Linear Regression Analysis* ,J.Wiley & Sons, New York, 1982.
6. M.Paunovic, in: *Electrochemistry in Transition* (O.J.Murphy, S.Srinivasan, and B.Conway, eds), Plenum Press, New York, 1992.
7. J.Duffy, L.Pearson, and M.Paunovic, *J.Electrochem.Soc.*, 130(1983)876.
8. M.Paunovic and D.Vitkavage, *J.Electrochem.Soc.*, 126(1979)2282.

Table I

The design matrix for 2^2 factorial experiments.
Matrix: orthogonal, symmetric.

Run (Combination)	Variable (Factor)	
	A	B
1	1	1
2	1	2
3	2	1
4	2	2

Factor levels:
1-low
2-high

Table II

The design matrix for 3^2 factorial experiments.
Orthogonal array.

Run (Combination)	Variable (Factor)	
	A	B
1	1	1
2	1	2
3	1	3
4	2	1
5	2	2
6	2	3
7	3	1
8	3	2
9	3	3

Table III

The central composite rotatable design matrix

(1) Fisher Matrix
16 Trial-5 variables
Factorial Design

A	Variable (Factor)			
	B	C	D	E
-1	-1	-1	-1	1
1	-1	-1	-1	-1
-1	1	-1	-1	-1
1	1	-1	-1	1
-1	-1	1	-1	-1
1	-1	1	-1	1
-1	1	1	-1	1
1	1	1	-1	-1
-1	-1	-1	1	-1
1	-1	-1	1	1
-1	1	-1	1	1
1	1	-1	1	-1
-1	-1	1	1	1
1	-1	1	1	-1
-1	1	1	1	-1
1	1	1	1	1

(2) Star points

A	B	C	D	E
-2	0	0	0	0
+2	0	0	0	0
0	-2	0	0	0
0	+2	0	0	0
0	0	-2	0	0
0	0	+2	0	0
0	0	0	-2	0
0	0	0	+2	0
0	0	0	0	-2
0	0	0	0	+2

(3) Center points (located at 00000), six experiments

Table IV
 Analysis of Variance on Mean
 3² Design

SOURCE OF VARIATION	DEGREES OF FREEDOM	SUM OF SQUARES	MEAN SQUARE	F	PROB	CONTRIB PERCENT
1 A citrate	2	28.617	14.309	10.304	.10	33
2 B boric acid	Pooled					
3 I_A citra_B boric	2	15.851	7.925	5.707	.15	17
4 I_A citra ² _B boric	2	30.781	15.350	11.054	.09	36
ERROR	2	2.777	1.389			14
TOTAL	8	77.95				

POOLED FACTORS FOR ERROR = Bboricacid

Table V

Estimated coefficients for the approximating polynomial

Variables	COEF	SE	T-STAT	P-VAL.	95% CONFIDENT	
					LOWER	UPPER
CONSTANT	-1756.347	525.421	-3.343	0.001	-702.503	-2810.192
XA	9.568	7.895	1.212	0.231	25.404	-6.267
XB	-52.923	10.065	-5.258	0	-32.736	-73.11
XC	-4.941	0.499	-9.907	0	-3.941	-5.941
XD	589.41	119.396	4.937	0	828.884	349.935
XE	-7.586	2.776	-2.733	0.008	-2.018	-13.154
XA XA	-0.101	0.073	-1.381	0.173	0.046	-0.248
XA XB	0.27	0.118	2.294	0.026	0.507	0.034
XA XC	0.008	0.006	1.42	0.161	0.02	-0.003
XA XD	-0.996	0.944	-1.056	0.296	0.897	-2.89
XA XE	-0.032	0.031	-1.037	0.304	0.03	-0.095
XB XB	-0.319	0.126	-2.541	0.014	-0.067	-0.571
XB XC	0.027	0.007	3.665	0.001	0.043	0.012
XB XD	5.801	1.178	4.922	0	8.164	3.437
XB XE	0.105	0.04	2.63	0.011	0.185	0.025
XC XC	-0.001	0	-4.774	0	-0.001	-0.002
XC XD	0.532	0.06	8.87	0	0.653	0.412
XC XE	0.006	0.002	3.21	0.002	0.01	0.002
XD XD	-44.274	7.305	-6.061	0	-29.623	-58.926
XD XE	0.663	0.32	2.07	0.043	1.305	0.02
XE XE	0.011	0.008	1.392	0.169	0.028	-0.005

SE, mean square error (1,5)

T, the test statistic (1)

p, level of significance of statistical test (4); any coefficient with p value less than 0.01 is significant

Table VI
 The experimental range, the center points,
 and the points of the minimum variability
 for process variables

Variable (Factor)	Experimental range	Center of range	Minimum variability
A	5.0-10.0	7.5	8.13
B	6.0-10.0	8.0	8.6
C	20-100	60.0	45.5
D	7.75-8.25	8.00	8.05
E	65-80	72.5	75.0

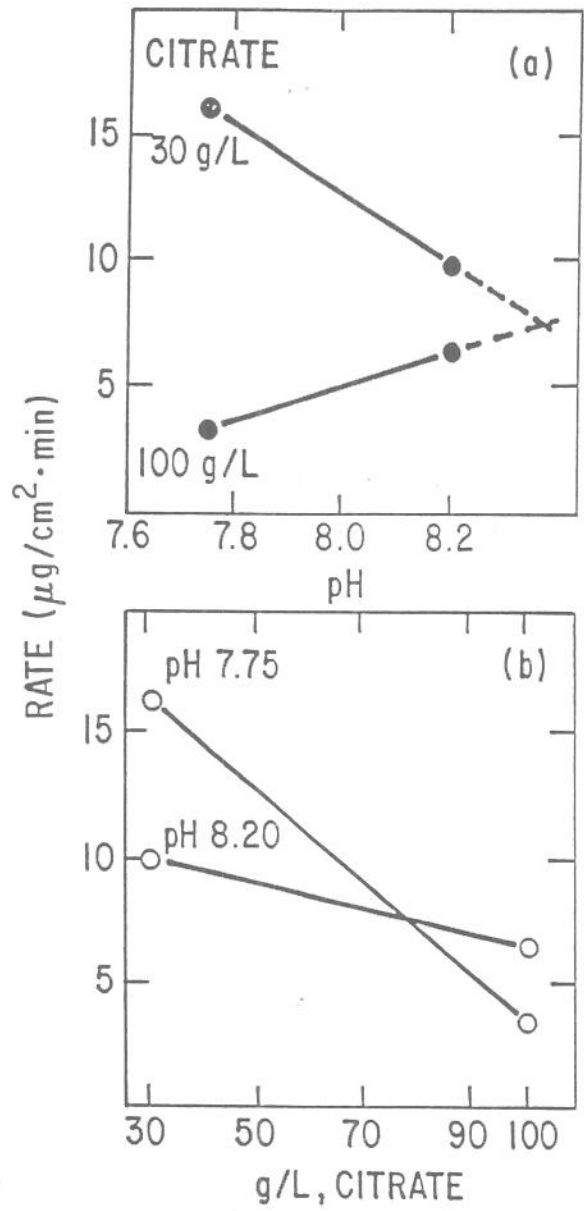


Fig.1. Interaction graph for citrate and pH determined by the design shown in Table I.

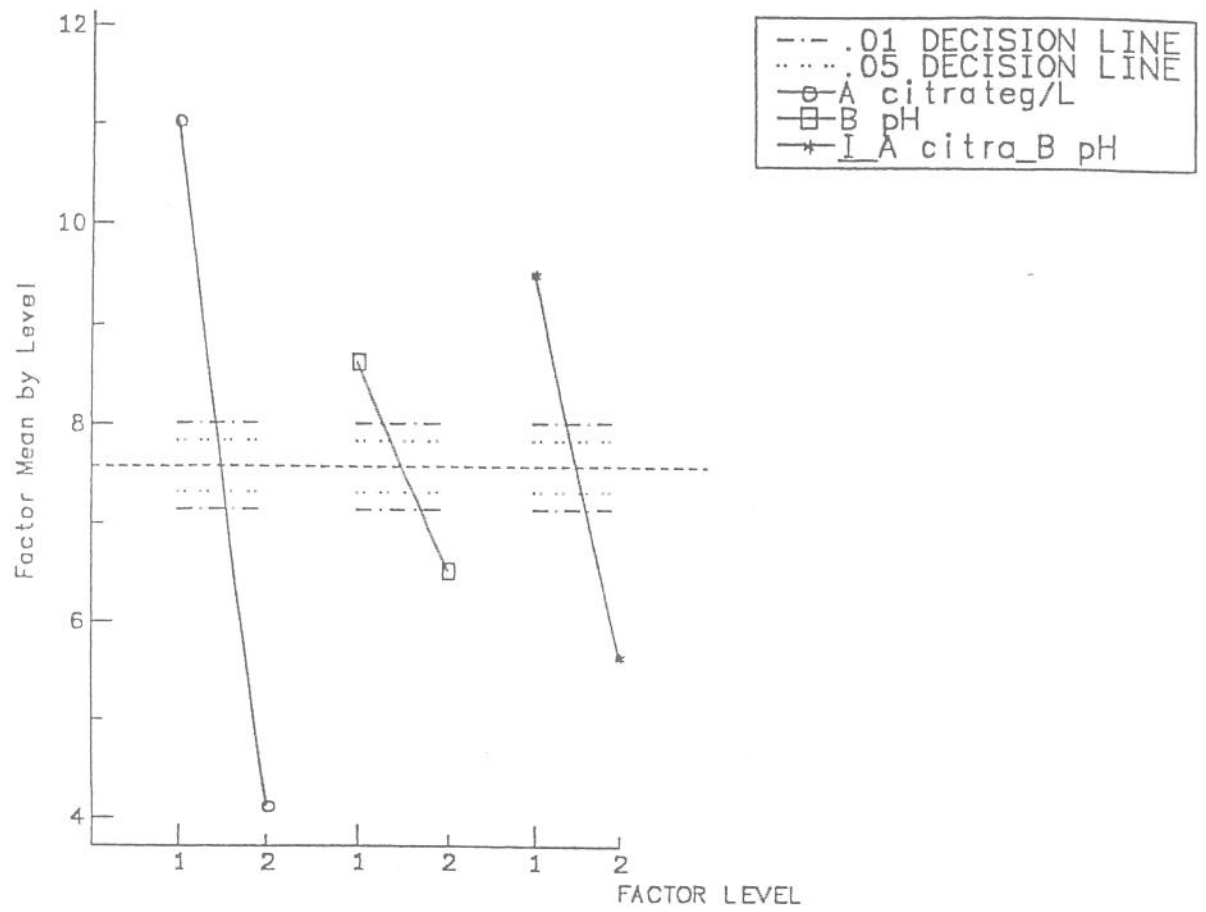


Fig.2. Analysis of means plot for the design shown in Table I with variables values given in Fig. 1.

DESIGN OF EXPERIMENT : DEPO RATE

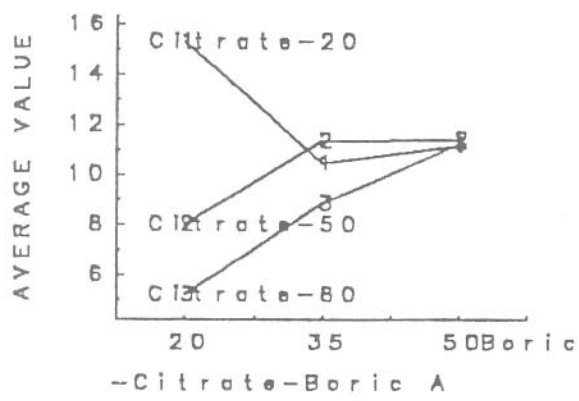


Fig.3. Interaction graph for citrate and boric acid determined by the design shown in Table II.

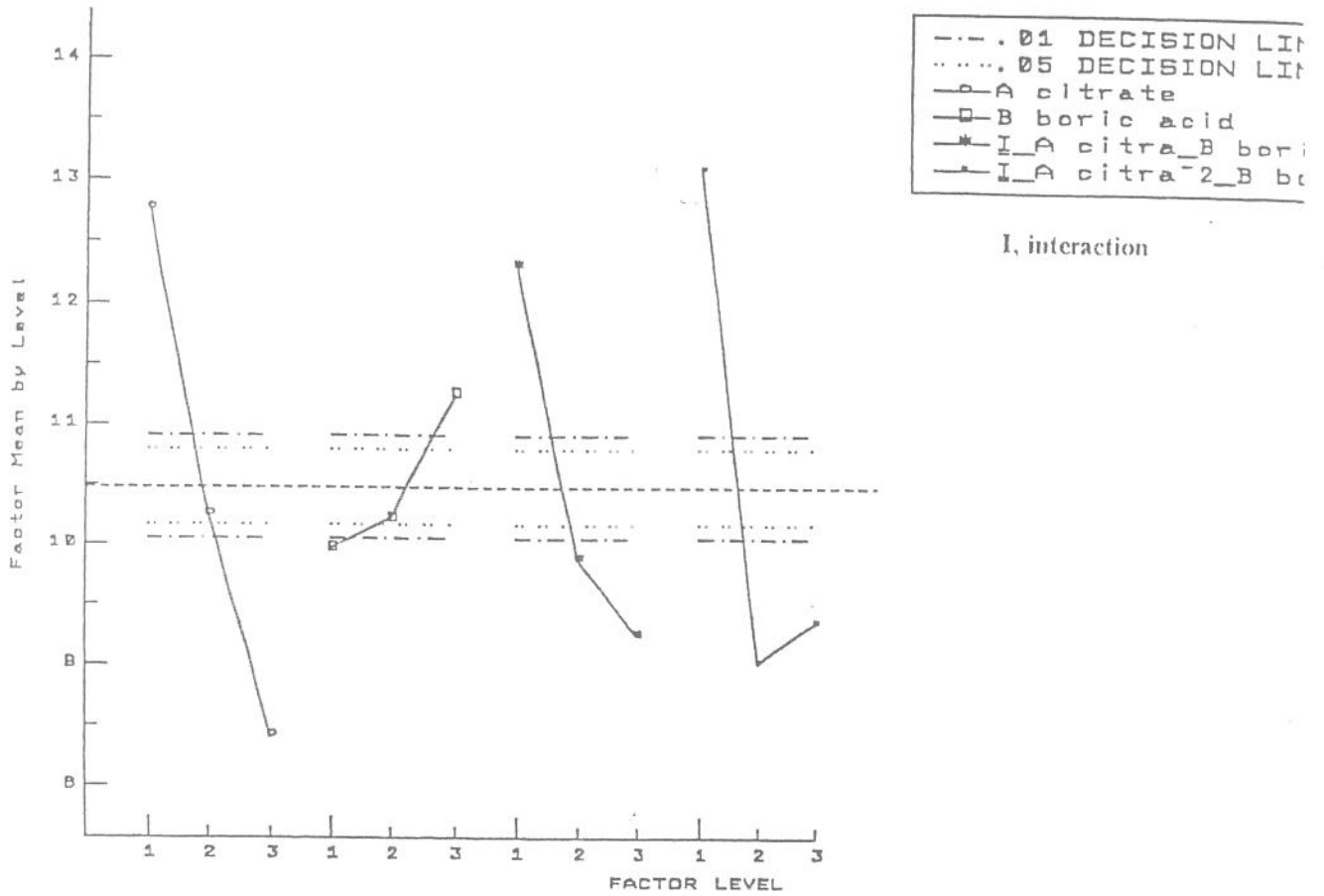


Fig.4. Analysis of means plot for the design shown in Table II with variables values given in Fig.3.

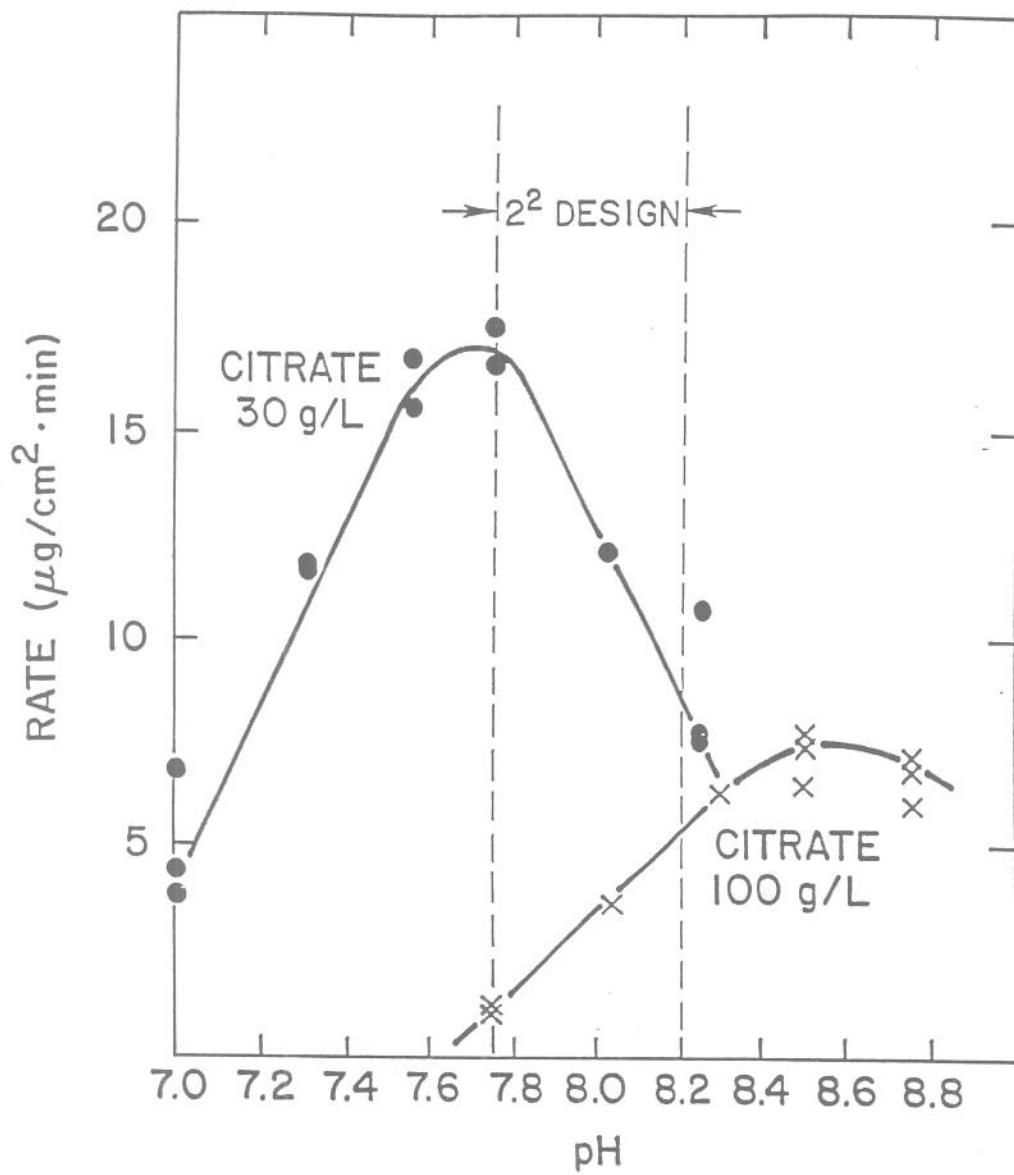


Fig.5. Rate of deposition as a function of pH at 30 and 100 g/L citrate.

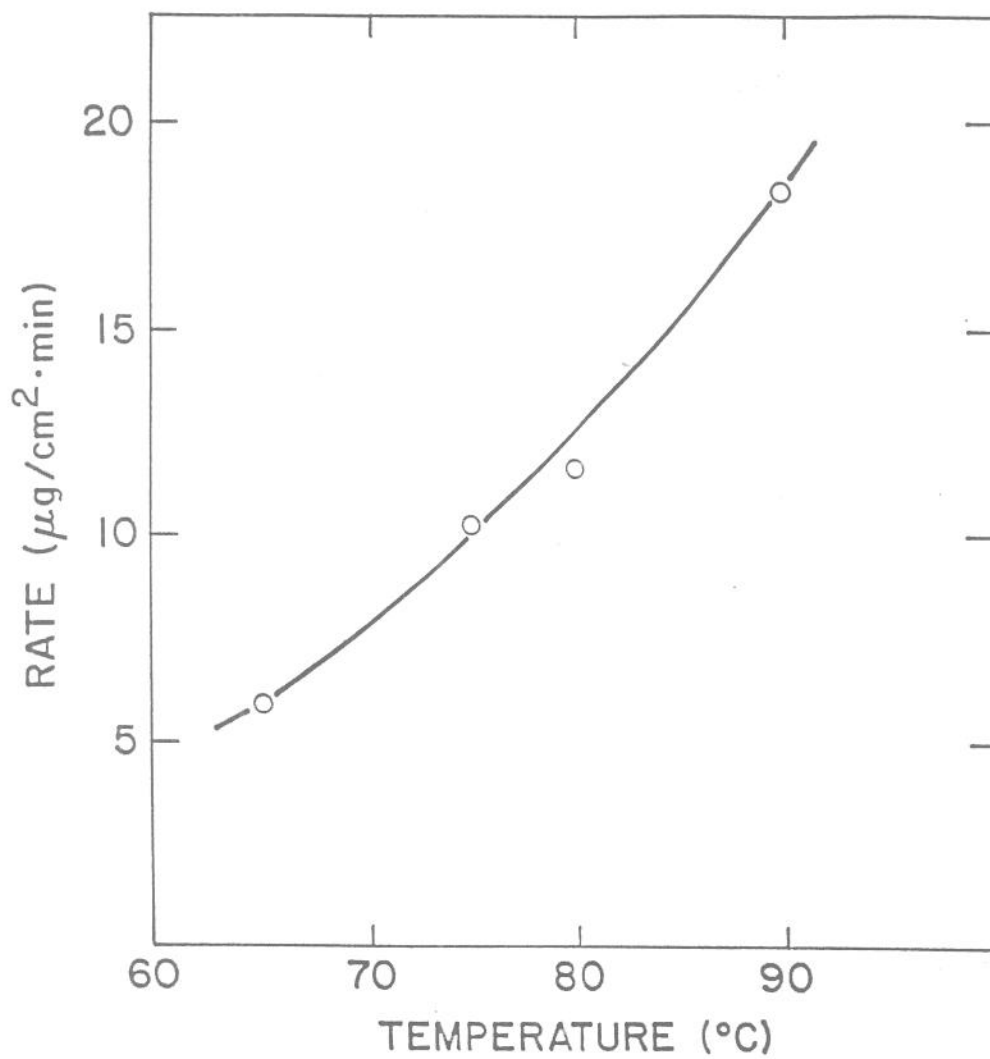


Fig.6. Rate of deposition as a function of temperature.

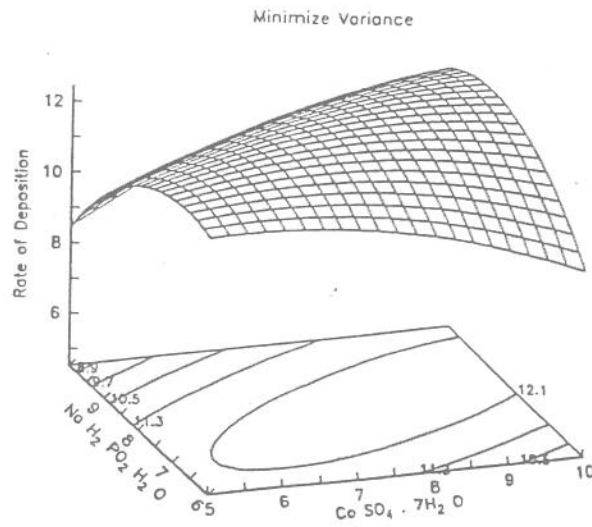
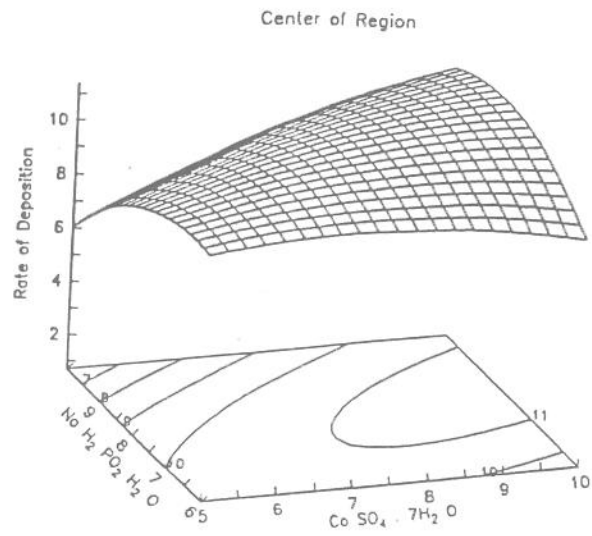


Fig.7. Response surfaces for the rate of deposition (in $\mu\text{g}/\text{cm}^2\cdot\text{min}$) as function of the concentration of cobalt sulfate and hypophosphite (in g/L).

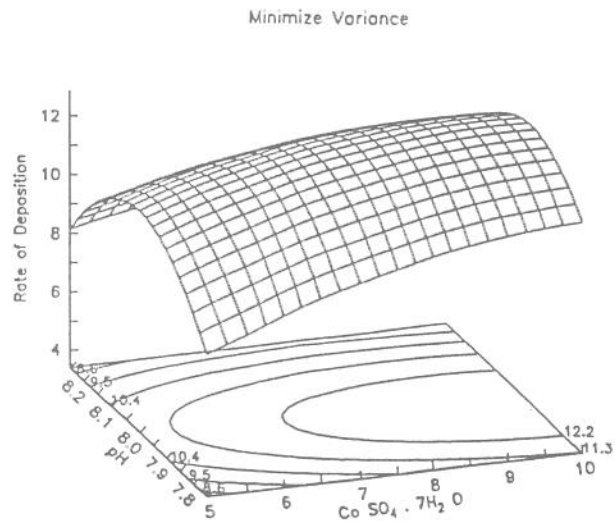
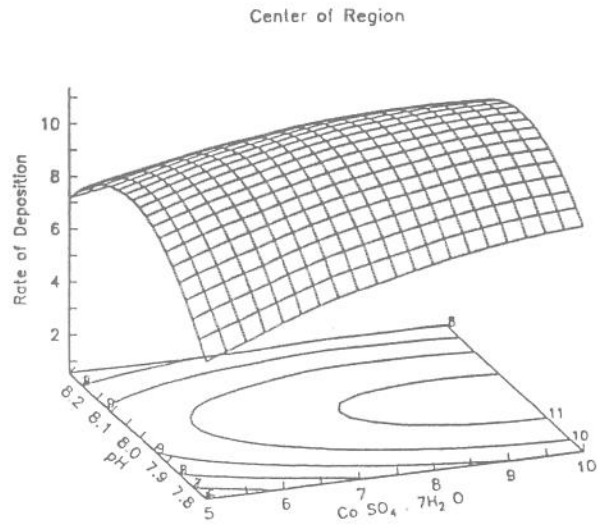


Fig.8. Response surfaces for the rate of deposition (in $\mu\text{g}/\text{cm}^2\cdot\text{min}$) as a function of the concentration of cobalt sulfate (in g/L) and pH.

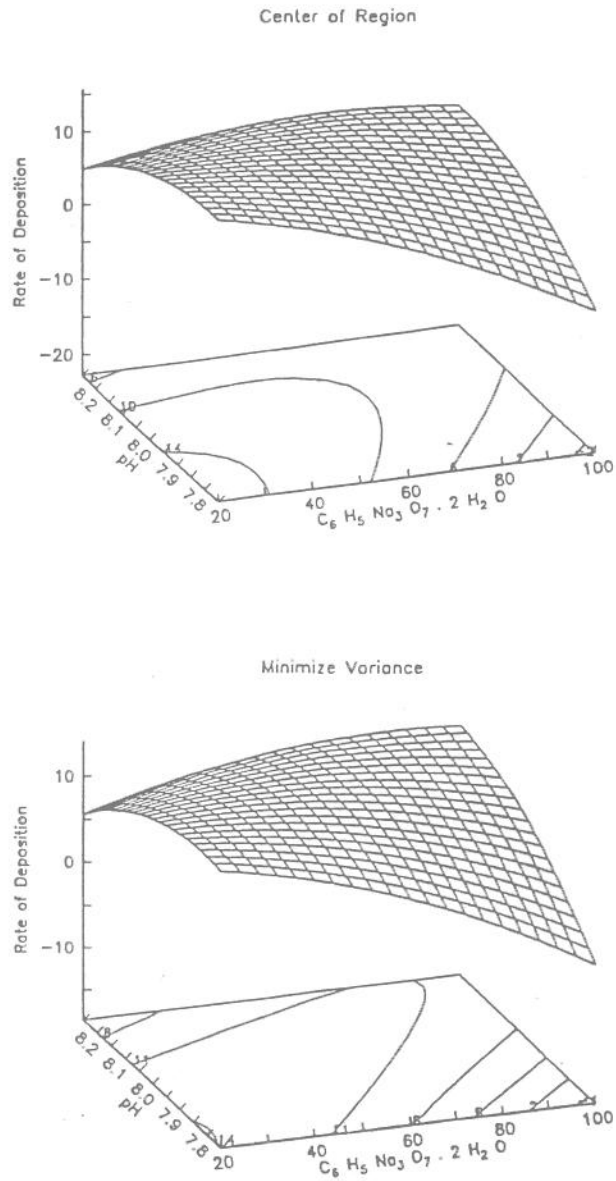


Fig.9. Response surfaces for the rate of deposition (in $\mu\text{g}/\text{cm}^2\cdot\text{min}$) as a function of the concentration of citrate (in g/L) and pH.

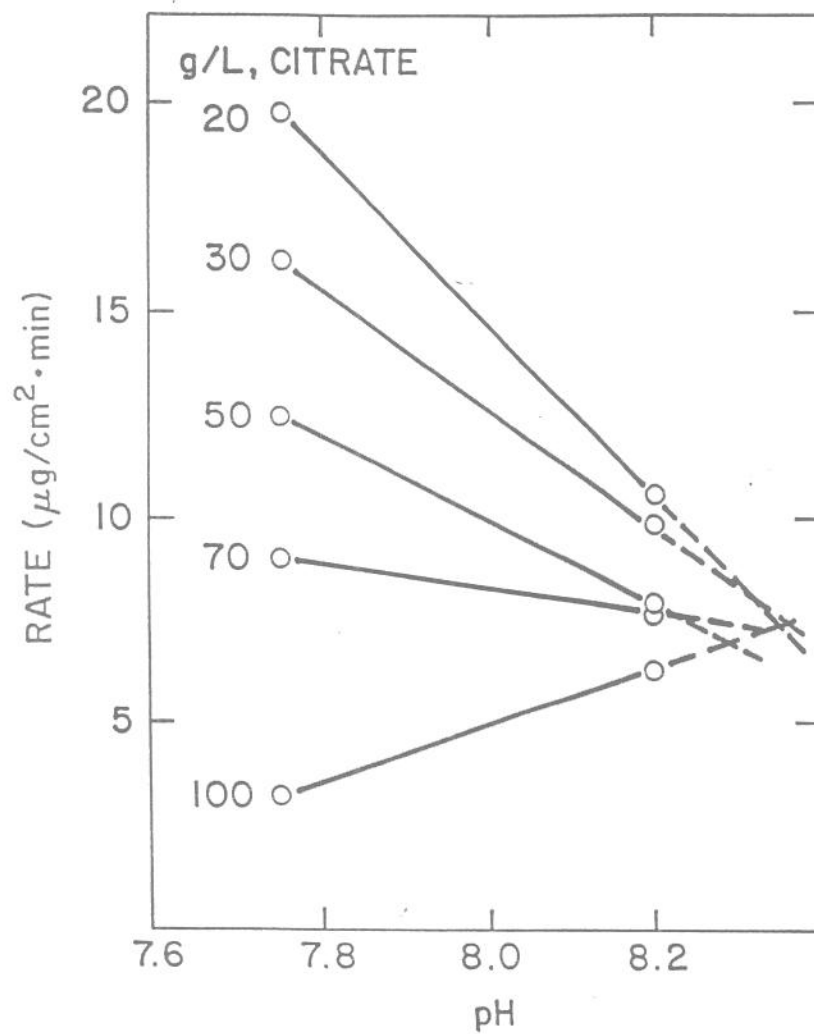


Fig.10. Rate of deposition as a function of pH at different concentrations of citrate.

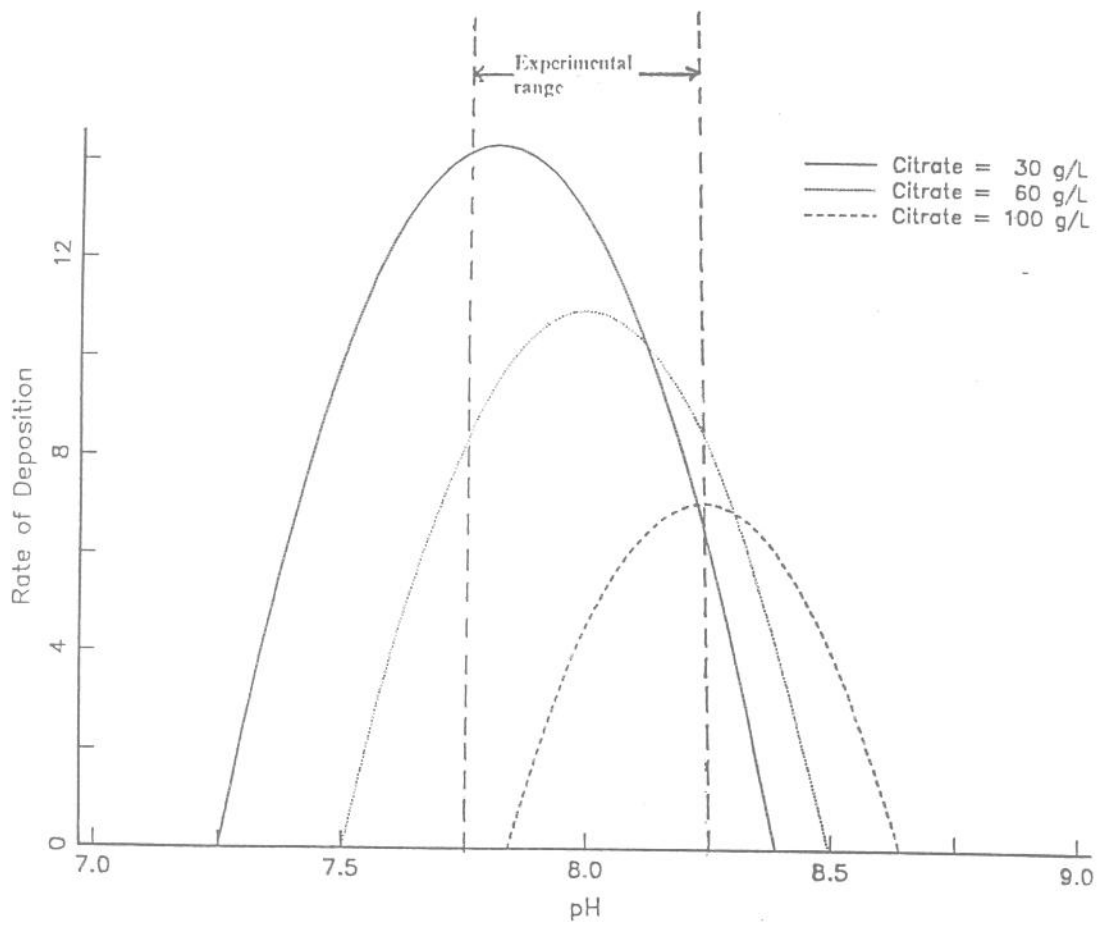


Fig.11. Extended approximating polynomials for the rate of deposition as a function of pH at different concentrations of citrate.